Rice canopy biochemical concentration retrievals based on Hyperion data

CHEN Jun-ying[1,2], TIAN Qing-jiu[1], QI Xue-yong[2], LIU Xiao-chen[1], GUAN Zhong[1]

1. *International Institute for Earth System Science, Nanjing University, Jiangsu Nanjing* 210093, *China*;
2. *China Centre for Resources Satellite Data & Application, Beijing* 100073, *China*

Abstract: The method of plot experiment with field application was used in this research. The variations of rice foliage and canopy spectra with corresponding biochemical concentration field-measured in jointing, heading and filling stages were analyzed. Through the analysis of absorption characteristic and vegetation index, the best spectral features for rice nitrogen and chlorophyll concentration estimation were obtained. Based on the Hyperion image of Jiangyan, we built the models of rice canopy nitrogen and chlorophyll estimation. At last, rice canopy nitrogen and chlorophyll concentration were retrieved from Hyperion image and their distribution maps were obtained. The results showed that: (1) Nitrogen concentration can be retrieved accurately using the area of absorption feature centered at 670nm based on band depth normalized to band depth (BNC) analysis; (2) Based on reversional normalized spectrum, NDVI using 560nm and 670nm was strongly correlated with chlorophyll concentration.

Key words: hyperspectral remote sensing, rice, Hyperion, nitrogen, chlorophyll

CLC number: TP79 **Document code:** A

1 INTRODUCTION

Precision agriculture is the world trend of agricultural development, and also an important way for agricultural sustainable development (Liu, 2002). Through the application of 3S technology, the space and time difference information of environmental factors related with crop growth can be collected and processed, and the management can be accurately adjusted, and then the maximum yield and economic efficiency can be obtained without environmental damage (Zhu *et al.*, 2000).

Rice is one of the main food crops in China. Biochemical parameters are good indicators of rice growth status. For example, nitrogen concentration is the important guiding factor of rice fertilization, while chlorophyll concentration can reflect the situation of rice photosynthesis. Real-time monitoring of changes in rice canopy biochemical concentration can help us to understand the growth of large area rice in time, and it is an important aspect of precision agriculture (Li, 2003).

Hyperspectral remote sensing has the characters of high spectral resolution and good continuity of bands, which can provide more spectral information. The development of hyperspectral remote sensing provides a powerful tool for quantitatively analyzing the relationship of biochemical concentration and spectral features. At present there are many methods for biochemical concentration retrievals, but most of them are based on the field measured spectra. Even if the remote sensing images were used, most of them are aerial images such as HyMap, AVIRIS, OMIS and so on. There are not many articles describing the rice biochemical concentration quantitative retrieval and mapping based on hyperspectral satellite imagery.

This study was based on spaceborne hyperspectral remote sensing technology and take precision agriculture as the application target. Rice foliage, canopy spectra and biochemical concentration (nitrogen & chlorophyll) of different species, growth conditions and at different growth stages were analyzed to research on the correlation model between spectral features and biochemical concentration. Furthermore, quantitative extraction and mapping technologies of rice canopy biochemical concentration based on hyperspectral remote sensing information were studied.

2 DATA SOURCES

2.1 Research area

The method of plot experiment with field application was used in this research. The study site is located at Yangzhou University (119°24′52.9″E, 32°23′36.9″N), in Jiangsu province, China. The total area is 715m^2. Yangzhou is located in the centre of Jiangsu province, the north shore of the Yangtze River and the southern end of the Jianghuai plain. Yangzhou has high index of land reclamation. The soil fertility and productivity of Yangzhou are relatively high in Jiangsu province. Rice planted

Received: 2007-06-10; **Accepted**: 2008-04-03

Foundation: Jiangsu Povince High Tech Research Projects (No.BG2004321 and No. BG2006340).

First author biography: CHEN Jun-ying(1983—), female, master. She graduated form Nanjing University, and is engaged in research of hyperspectral remote sensing. She has published 5 papers. E-mail: cjy831025@163.com.

in this field included two typical varieties: Changyou 1 and Wujing 15. Nitrogen application from 0 to 25 kg was divided into 8 levels. There are two same series and 32 plots.

The field covered by Hyperion image for application was located in Jiangyan area, Jiangsu province. Jiangyan has been called granary since ancient times. Jiangya teemed with rice and it is the commodity grain base of China. We selected eight paddy fields of image covering area as sampling sites. Synchronously with the image acquisition, field-based canopy reflectance spectra, nitrogen and chlorophyll concentration were recorded at those eight sites. The latitudes and longitudes of those sites were accurately measured by GPS, in order to precisely locate the sites in the image. Fig. 1 shows the image coverage and sampling sites distribution.

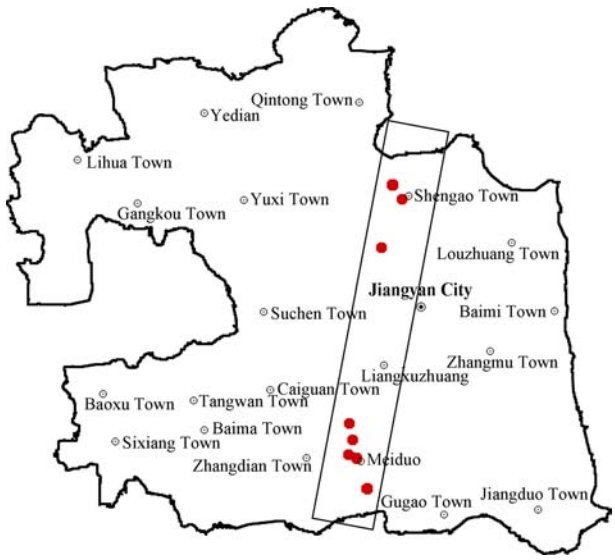

Fig. 1 The image coverage and sampling sites distribution

2.2 Field spectra measurement

The foliage and canopy reflectance spectra were collected with ASD FieldSpec Pro FR spectroradiometer. The wavelength range is from 350 to 2500 nm. Sampling interval between 350 and 1000 nm is 1.4 nm, between 1000 and 2500 nm is 2 nm.

Rice canopy reflectance spectra were collected when the sky was clear. Probe perpendicular to the canopy, and the distance between probe and rice canopy was about 0.5 m, 25 ° visual field was used. We selected 3—5 sample points in every plot and collected 2—3 spectra for every sample point. All of the spectra collected in one plot were averaged to obtain the canopy spectrum of that plot.

We collected 5 rice leaves of every plot in Yangzhou experimental field, 10 rice leaves of every plot in Jiangyan field for foliage spectra measurement. The foliage spectra were collected in darkroom. The reflectance spectrum of every leaf was acquired by averaging the spectra of 4—6 measurements.

This study was from August 15 to September 30, 2005, involved jointing, heading and filling stages. 1225 canopy spectra and 2925 foliage spectra were collected. As shown in Table 1, we measured the canopy and foliage reflectance spectra in Yangzhou experimental field on August 15, September 6 and September 30, 2005. Synchronously with the image acquisition, field-based canopy reflectance spectra were recorded at 8 sample plots in Jiangyan field on September 7, 2005.

Table 1 Spectra field-measurement in 2005

Date	August 15	September 6	September 7	September 30
Location	Yangzhou experimental field	Yangzhou experimental field	Jiangyan field	Yangzhou experimental field
Growth stage	Jointing stage	Heading stage	Heading stage	Filling stage.
Sample number	160	192	—	160
Canopy spectra number	324	289	128	484
Foliage spectra number	960	1000	—	965

2.3 Nitrogen and chlorophyll concentration measurement and treatment

Nitrogen and chlorophyll concentration was immediately measured after the spectra acquisition. Nitrogen concentration was measured through kjeldahl nitrogen method. Chlorophyll concentration was measured by using the SPAD-502 instrument. The SPAD-502 instrument can measure foliage chlorophyll concentration without destruction. It determines foliage chlorophyll relative concentration according to the absorptivity of two wavelength ranges (Pu & Gong, 2000). The chlorophyll concentration was acquired by averaging the values of 6 to 10 measurements. The nitrogen and chlorophyll concentration of every plot was determined by averaging all the values of leaves sampled from the plot.

2.4 Hyperion data acquisition

The Hyperion sensor is the first civilian spaceborne hyperspectral instrument. It acquire visible near-infrared (VNIR) and shortwave infrared (SWIR) spectra by push broom technique. Hyperion data have 242 bands and the main characteristics are shown in Table 2.

The Hyperion data was acquired at 10:20 A.M. on Sep 7, 2005, with a size of 255×3471 pixels. The image covered Jiangyan area, Jiangsu province and was centered at 120°8′2″E, 32°29′6″N.

Table 2 Main characteristics of Hyperion data (Richard, 2003)

Wavelength range/nm	356—2577
Number of bands	242
Spatial resolution/m	30
VNIR bands	1—70 (356—1058nm)
SWIR bands	71—242 (852—2577nm)
Data type	2-byte singed integer

3 HYPERION IMAGE PROCESSING

3.1 Hyperion image preprocessing

Hyperion image preprocessing included eliminating uncalibrated and atmospheric water vapor affected bands, absolute radiometric calibration, stripes and "smile" effect removal, atmospheric correction and spectrum smoothing. At last, the reflectance image was obtained.

A number of bands were uncalibrated and others had low sensitivity of the spectrometer materials. Because of this, only 166 bands were used in this study. The remain bands and wavelengths are shown in Table 3.

Table 3 The remain wavelengths of Hyperion image

Hyperion original bands	Wavelengths/nm
8—54	426—895
80—119	943—1336
131—164	1457—1790
180—224	1952—2396

The SWIR bands have a scaling factor of 80 and the VNIR bands have a scaling factor of 40 applied (Richard, 2003). Every band dividing by the scaling factor can generate the absolute radiometric calibrated image.

Global equalization was used to remove the stripes and "smile" effect. It thought that the mean value and standard deviation of each column in each band were the same. The mean value and standard deviation of each column were modified to match those for the whole image for each band.

The image was corrected for atmosphere with the Fast Line-of-sight Atmospheric Analysis of Spectral Hypercubes (FLAASH) to retrieve the ground reflectances. FLAASH is a first-principles atmospheric correction modeling tool for retrieving spectral reflectance from hyperspectral images. It made the obscuring effects of the atmosphere accurately removed.

After a series of processing, the deficiencies and uncertainties of every step lead to the continuous noise of atmospheric corrected image spectra. The noise may exert an adverse effect on the quantitative application of image. An inverse minimum noise fraction (MNF) transformation was applied to the FLAASH-derived surface reflectance image to separate noise from the data (Datt *et al.*, 2003).

The atmospheric corrected image reflectances were quite similar to the field measured canopy reflectances (Fig. 2). The result of spectral rebuilt was satisfactory.

3.2 Geometric correction

The geometric correction was through applying 22 GCPs collected from 1:50000 relief maps covering the study area to the reflectance image. The total error was less than one pixel.

3.3 Discrimination of paddy rice fields

The research subject of this paper is rice, so we discriminated paddy rice field from the image for rice biochemical concentration analysis and retrieval. It was also help for identifying the results more easily.

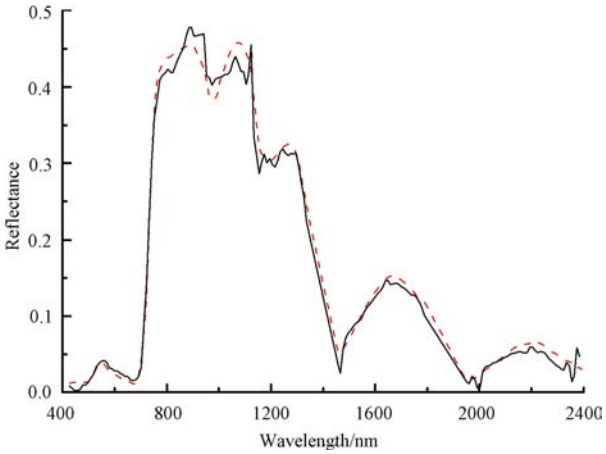

Fig. 2 Comparison between Hyperion reflectance spectrum and field measured canopy spectrum

Firstly, vegetation was extracted with normalized difference vegetation index (NDVI). NDVI is given by the formula:

$$\mathrm{NDVI}=\frac{\rho_{\mathrm{NIR}}-\rho_{\mathrm{RED}}}{\rho_{\mathrm{NIR}}+\rho_{\mathrm{RED}}} \tag{1}$$

where ρ_{RED} and ρ_{NIR} are the reflectance of red and near infrared bands. We applied the threshold (NDVI$\geq$0.7) to identify vegetation pixels.

Then we calculated Enhanced Vegetation Index (EVI) and Surface Water Index (LSWI) of the image (Huete *et al.*, 2002). EVI and LSWI are given by the formulas:

$$\mathrm{EVI}=2.5\times\frac{\rho_{\mathrm{NIR}}-\rho_{\mathrm{RED}}}{\rho_{\mathrm{NIR}}+6\times\rho_{\mathrm{RED}}-7.5\times\rho_{\mathrm{BLUE}}+1} \tag{2}$$

$$\mathrm{LSWI}=\frac{\rho_{\mathrm{NIR}}-\rho_{\mathrm{SWIR}}}{\rho_{\mathrm{NIR}}+\rho_{\mathrm{SWIR}}} \tag{3}$$

where ρ_{BLUE}, ρ_{RED}, ρ_{NIR} and ρ_{SWIR} are the reflectance of blue, red, near infrared and shortwave infrared bands. The Hyperion image was acquired at the heading stage of rice and the leaf area index was relatively higher at that time. As we know when the vegetation coverage more than 80%, the NDVI values increase with delay and become saturation, so in this study we chose Enhanced Vegetation Index (EVI) to identify rice from other vegetation. EVI directly adjusts the reflectance in the red band as a function of the reflectance in the blue band, and it accounts for residual atmospheric contamination and variable soil and canopy background reflectance (Huete *et al.*, 1997, 2002). The EVI values of paddy rice fields were lower than other vegetation fields. The distinct differentiate between paddy rice fields and other vegetation fields is that the rice is grown on flooded soils, so we used LSWI which was sensitive to the leaf water and soil moisture. The LSWI values of paddy rice fields were higher than other vegetation fields. Thus it can be seen as to paddy rice fields, the values of EVI–LSWI were lower than other vegetation fields. In this study, the paddy rice

field pixels were identified by using the threshold of EVI–LSWI≤0.24.

Fig. 3 shows the comparison between original pseudo-color composite image and paddy rice image. As the original pseudo-color composite image of Fig. 3(a) shows, paddy rice fields are presented as dark red and other vegetation fields are presented as bright red. Paddy rice fields are presented as white in Fig. 3(b). The accuracy of paddy rice field discrimination was evaluated with 3812 non-vegetation samples, 272 rice samples and 2483 other vegetation samples. We established confusion matrix and computed some correlative data. The accuracy of paddy rice field discrimination is shown in Table 4. The overall accuracy of paddy rice field discrimination is 92.89% and the kappa is 0.8915. The result showed that the method of paddy rice field discrimination was relatively accuracy and feasible.

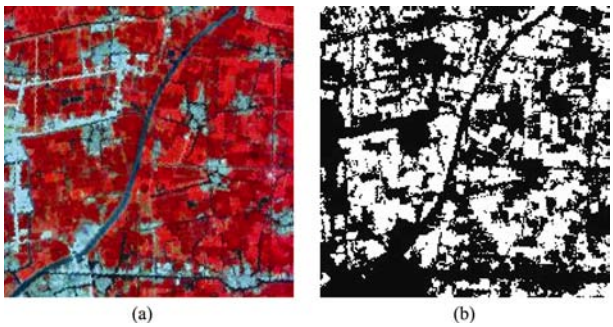

Fig. 3 Comparison between original pseudo-color composite image and paddy rice image
(a) Original pseudo-color composite image; (b) Paddy rice image

Table 4 Rice discrimination accuracy

Type	Non-vegetation	Rice	Other vegetation	Sum	User accuracy/%
Non-vegetation	3701	16	15	3732	99.17
Rice	70	2563	353	2986	85.83
Other vegetation	41	146	2115	2302	91.88
Sum	3812	2725	2483	9020	—
Producer accuracy/%	97.09	94.06	85.18	—	—
Overall accuracy=92.89% Kappa coefficient=0.8915					

4 METHODS

4.1 Method based on spectral absorption feature

The method was based on the thought of continuum removal can remove those background influence and thus to isolate individual absorption features. The continuum is a straight line fitted over the top of a spectrum that connects local spectral maxima. The continuum-removed reflectance is calculated by dividing the original reflectance values by the reflectance of continuum at the corresponding wavelength (Shi *et al.*, 2005). Based on the continuum removal, the spectral transformation of band depth normalized to band depth at the centre of the absorption feature (BNC) and the area of absorption feature (BNA) were used.

4.1.1 Band depth normalized to band depth at the centre of the absorption feature (*BNC*)

The normalized band depths (BNC) are calculated by dividing the band depth of each band by the band-depth at the band center:

$$\mathrm{BNC} = (1-(R/R'))/(1-(R_c/R_c')) \quad (4)$$

where R is the reflectance of each wavelength, R' is the reflectance of continuum at the corresponding wavelength, R_c is the reflectance of the absorption feature centre wavelength, R_c' is the reflectance of continuum at the absorption feature centre wavelength.

4.1.2 Band depth normalized to area of absorption feature (*BNA*)

The band depths normalized to area (BNA) are calculated by dividing the band depth of each band by the area of the absorption feature:

$$\mathrm{BNA} = (1-(R/R'))/A \quad (5)$$

where A is the area of the continuum-removed absorption feature.

4.1.3 Selection of spectral absorption feature band

In this study, we used two band selection methods:

(1) We applied continuum-removal analysis to the whole spectrum of each sample. As shown in Fig. 4 and Fig. 5, the continuum-removal spectrum produced four isolated wavelength ranges centered at 670, 980, 1160 and 1950nm.

(2) We selected 6 wavelength ranges according to the rice original reflectance spectrum and the known chlorophyll and nitrogen absorption feature (Table 5). We consulted the result of absorption features listed by Curran (1989). The nitrogen absorption feature bands are 910, 1020, 1510, 1980, 2060, 2130, 2180, 2240, 2300 and 2350nm, the chlorophyll absorption feature bands are 460, 640 and 660nm.

In this study, we analyzed the correlation of nitrogen and chlorophyll concentration with the depth, width and area of BNC and BNA absorption feature.

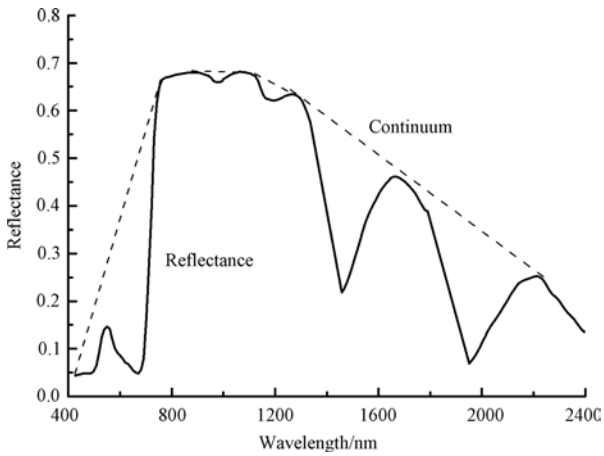

Fig. 4 A reflectance spectrum and its continuum

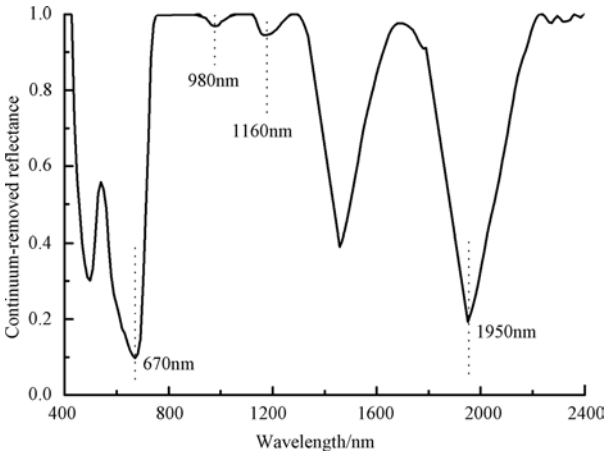

Fig. 5 A continuum-removed spectrum and the band centers

4.2 Method based on vegetation indices

We consulted some literatures and selected 6 vegetation indices shown in Table 6 according to the rice spectral features. We used the spectral transformation of 1 minus continuum-removed spectra and reversional normalized spectra were obtained. We calculated the 6 vegetation indices based on original spectra, normalized spectra and reversional normalized spectra. The correlation coefficients between biochemical concentration (nitrogen and chlorophyll) and vegetation indices can be obtained.

Table 5 Selected wavelength ranges and their associated absorption features for nitrogen and chlorophyll

Known chlorophyll and nitrogen absorption features/nm	Selected wavelength/nm
460	436.99—548.92
640, 660	569.27—762.6
910, 1020	894.7—1083.99
1510	1285.76—1648.91
1980, 2060, 2130, 2180	1961.66—2203.83
2240, 2300, 2350	2224.02—2395.5

Table 6 Vegetation indices employed in this study

Vegetation index	Full name	Formula	Reference
NDVI560_670	Normalized difference vegetation index	$\mathrm{NDVI560\_670}=\frac{R_{560}-R_{670}}{R_{560}+R_{670}}$	Rouse *et al.*, 1974
RVI560_670	Ratio vegetation index	$\mathrm{RVI560\_670}=\frac{R_{560}}{R_{670}}$	Pearson & Miller, 1972
NRI	Nitrogen reflectance index	$\mathrm{NRI}=\frac{R_{570}-R_{670}}{R_{570}+R_{670}}$	Schleiche *et al.*, 2001
CARI	Chlorophyll absorption ratio index	$\mathrm{CARI}=\frac{\lvert a\times 670+R_{670}+b\rvert R_{700}}{\sqrt{a^2+1}\times R_{670}}$, $a=(R_{700}-R_{550})/150, b=R_{550}-550\times a$	Kim *et al.*, 1994
VARI_green	Visible atmospherically resistant index	$\mathrm{VARI\_green}=\frac{R_{560}-R_{670}}{R_{560}+R_{670}+R_{450}}$	Anatoly *et al.*, 2002
VARI_700	Visible atmospherically resistant index	$\mathrm{VARI\_700}=\frac{R_{700}-1.7\times R_{670}+0.7\times R_{450}}{R_{700}+2.3\times R_{670}-1.3\times R_{450}}$	Anatoly *et al.*, 2002

5 RESULT ANALYSIS

5.1 Selection of best spectral feature for rice nitrogen and chlorophyll concentration estimation

We analyzed the correlation between field spectra measured on August 15, September 6 and September 30 with biochemical concentration. The correlation coefficients between biochemical concentration with spectral features and vegetation indices were calculated.

Table 7 shows the spectral features significantly correlated with nitrogen concentration in the 3 growth stages. The spectral feature with maximum correlation coefficient is 670Area (BNC), which means the area of absorption feature centered at 670nm based on BNC analysis. So the 670Area (BNC) was chosen to be the best spectral feature for nitrogen concentration retrieval.

Table 8 shows the spectral features significantly correlated with chlorophyll concentration in the 3 growth stages. The spectral feature with maximum correlation coefficient is NDVI560_670 (reversional normalized spectrum), which means NDVI used 560nm and 670nm based on reversional normalized spectrum. So the NDVI560_670 (reversional normalized spectrum) was chosen to be the best spectral feature for chlorophyll concentration retrieval.

5.2 Rice canopy nitrogen and chlorophyll concentration retrievals and mapping based on Hyperion data

The above best spectral features for nitrogen and chlorophyll concentration retrievals based on field measured spectra study were applied to the Hyperion image reflectance of 8 fields. The rice canopy nitrogen and chlorophyll concentration retrieval models are:

$$N = 0.0357 \times 670\mathrm{Area(BNC)} - 7.0023 \quad (6)$$

CHL=207.16×NDVI560_670(reversional normalized spectrum)+ 15.772 (7)

The quadratic polynomial multiple correlation coefficient (R^2) between the 670Area (BNC) and nitrogen concentration is 0.79 (Fig. 6). The R^2 between the NDVI560_670 (reversional normalized spectrum) and chlorophyll concentration is 0.77 (Fig. 7).

Table 7 Spectral features significantly correlated with nitrogen concentration and the correlation coefficients

Spectral features	August 15		September 6		September 30	
	Foliage	Canopy	Foliage	Canopy	Foliage	Canopy
PSSRb (original spectrum)	0.55	0.55	0.56	0.44	0.74	0.61
PSNDb (original spectrum)	0.55	0.56	0.61	0.50	0.74	0.71
CARI (normalized spectrum)	0.67	0.61	0.62	0.52	0.77	0.74
NDVI560_670 (reversional normalized spectrum)	0.71	0.56	0.61	0.55	0.72	0.72
RVI560_670 (reversional normalized spectrum)	0.71	0.58	0.61	0.55	0.76	0.74
NRI (reversional normalized spectrum)	0.69	0.58	0.62	0.56	0.72	0.72
CARI (reversional normalized spectrum)	0.67	0.59	0.62	0.48	0.77	0.72
VARI_green (reversional normalized spectrum)	0.69	0.56	0.61	0.53	0.72	0.72
VARI_700 (reversional normalized spectrum)	0.69	0.55	0.66	0.49	0.76	0.74
670Area (BNC)	0.72	0.56	0.62	0.56	0.76	0.74
670Depth (BNA)	0.66	0.56	0.64	0.50	0.71	0.72
640, 660Depth (BNA)	0.64	0.61	0.49	0.55	0.83	0.74

Table 8 Spectral features significantly correlated with chlorophyll concentration and the correlation coefficients

Spectral features	August 15		September 6		September 30	
	Foliage	Canopy	Foliage	Canopy	Foliage	Canopy
PSNDb (original spectrum)	0.64	0.56	0.62	0.44	0.94	0.77
CARI (original spectrum)	0.71	0.67	0.66	0.53	0.96	0.85
NDVI560_670 (reversional normalized spectrum)	0.76	0.62	0.71	0.58	0.96	0.86
RVI560_670 (reversional normalized spectrum)	0.76	0.59	0.71	0.58	0.96	0.85
NRI (reversional normalized spectrum)	0.76	0.62	0.71	0.56	0.96	0.86
CARI (reversional normalized spectrum)	0.74	0.62	0.61	0.48	0.94	0.83
VARI_green (reversional normalized spectrum)	0.76	0.61	0.72	0.56	0.96	0.86
VARI_700 (reversional normalized spectrum)	0.76	0.53	0.66	0.48	0.96	0.85
670Depth (BNA)	0.74	0.58	0.71	0.52	0.96	0.86
640, 660Area (BNC)	0.76	0.61	0.67	0.48	0.94	0.79
640, 660Depth (BNA)	0.76	0.64	0.67	0.49	0.96	0.83

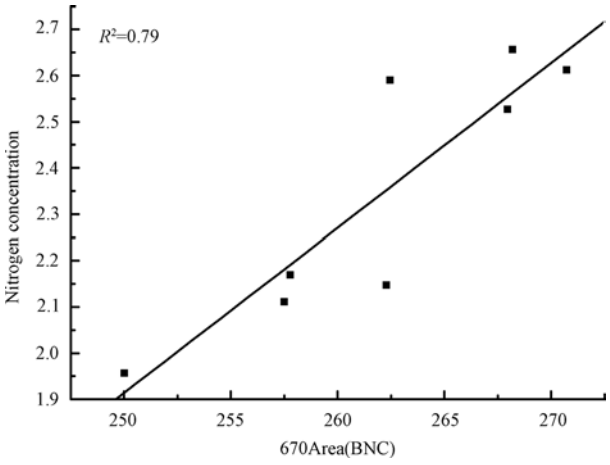

Fig. 6 Correlation between 670Area (BNC) based on image spectrum and nitrogen concentration

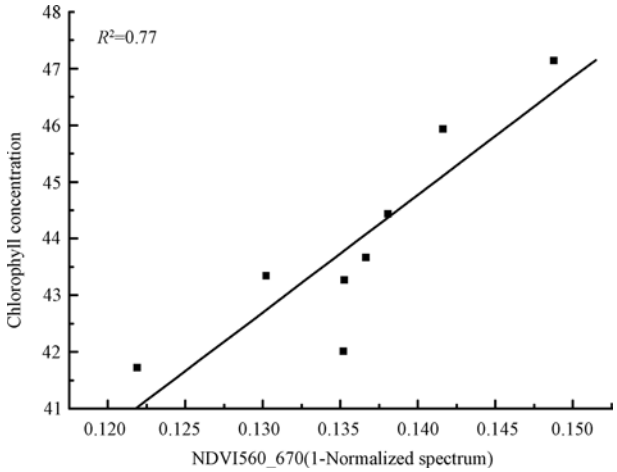

Fig. 7 Correlation between NDVI560_670 (1-Normalized spectrum) based on image spectrum and rice canopy chlorophyll concentration

We applied the two models on the Hyperion paddy rice image and produced the chlorophyll and nitrogen concentration distribution maps (Fig. 8, Fig. 9). The values of nitrogen concentration in nitrogen concentration distribution map ranged from 0.06 % to 4.46 % and the values of chlorophyll concentration in chlorophyll concentration distribution map ranged from

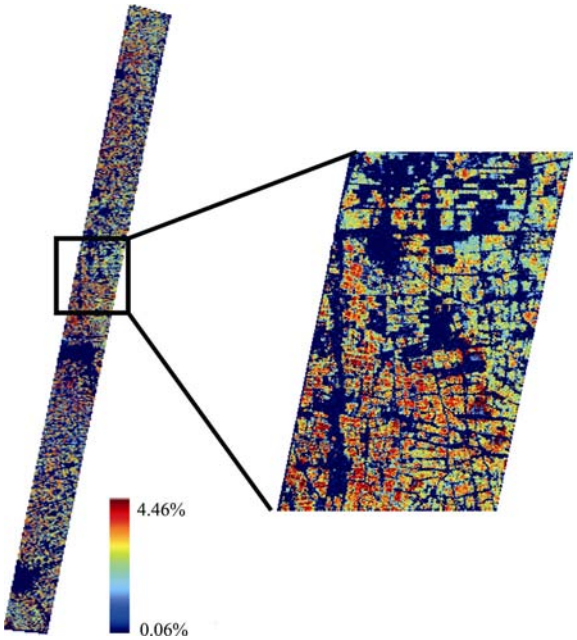

Fig. 8 Rice canopy nitrogen concentration distribution map

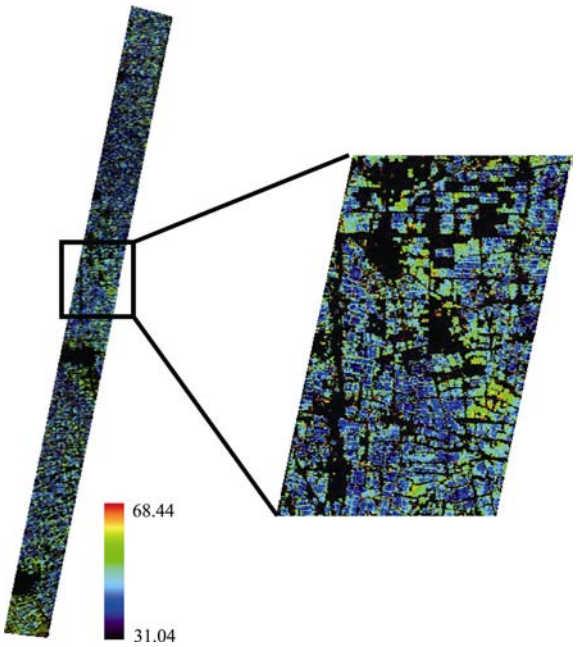

Fig. 9 Rice canopy chlorophyll concentration distribution map

31.04 to 68.44. They were quite consistent with those of field measurements. The pixel values in each field were relatively uniform. The distribution agreed highly with the growth status distribution. Therefore to some extent, the estimation equations were validated.

6 CONCLUSIONS

In this study, we analyzed the correlation between rice biochemical concentration (nitrogen and chlorophyll) with field measured foliage and canopy spectra of different species and different growth stages. Then we obtained the universal spectral features with high precision for rice nitrogen and chlorophyll concentration estimation based on field measured spectra analysis. The result of field measured spectra analysis was applied to Hyperion image and the nitrogen and chlorophyll concentration estimation models were established. The study investigated the feasible of nitrogen and chlorophyll concentration retrieval based on Hyperion image and retrieved the rice canopy nitrogen and chlorophyll concentration of research area. At last, the rice canopy nitrogen and chlorophyll concentration distribution maps were produced. The results include as follow:

(1) The area of absorption feature centered at 670nm based on BNC analysis was found to be strongly correlated with the nitrogen concentration of jointing, heading and filling stages both at foliage and canopy level. The rice canopy nitrogen concentration retrieval model was built based on spaceborne hyperspectral remote sensing image spectra using the spectral feature. The results showed that the correlation coefficient (R^2) between the area of absorption feature centered at 670nm based on BNC spectra and rice canopy nitrogen concentration was 0.79. The result of rice canopy nitrogen concentration retrieval was quite accurate and reliable.

(2) Based on the reversional normalized spectrum, 560nm and 670nm were used to establish NDVI560_670. The spectral feature was found to be strongly correlated with the chlorophyll concentration of jointing, heading and filling stages both at foliage and canopy level. The rice canopy chlorophyll concentration retrieval model was built based on spaceborne hyperspectral remote sensing image spectra using the spectral feature. The results showed that the R^2 between NDVI560_670 based on the reversional normalized spectra and rice canopy chlorophyll concentration was 0.77. The result was satisfactory.

The study taken rice as the research object, investigated the methods for nitrogen and chlorophyll concentration retrievals. Other vegetation types and biochemical parameters can be taken as the research objects in future. The results of this study can provide reference for estimation of crop yield and pests detection with hyperspectral remote sensing.

REFERENCES

Anatoly A, Gitelson Y, Yoram J K, Robert S and Don R. 2002. Novel algorithms for remote estimation of vegetation fraction. *Remote Sens. Environ*, **80**: 76—87

Curran P J. 1989. Remote sensing of foliar chemistry. *Remote Sensing of Environment*, **30**, 271—278

Datt B, McVicar T R, Van Niel T G, Jupp D L B and Pearlman J S. 2003. Pre-processing EO-1 hyperion hyperspectral data to support the application of agricultural indices. *IEEE Transactions on Geoscience and Remote Sensing*, **41**(6): 1246—1259

FLAASH Module User's Guide, ENVI FLAASH Version 4.2, August, 2005 Edtion

<http://www.jsyzagri.gov.cn/old/gkzr.htm.>

<http://jiangyan.soujz.com/.>

Huete A R, Liu H Q, Batchily K and VanLeeuwen W. 1997. A comparison of vegetation indices global set of TM images for EOSMODIS. *Remote Sensing of Environment*, **59**: 440—451

Huete A R, Didan K, Miura T, Rodriguez E P, Gao X and Ferreira L G. 2002. Overview of the radiometric and biophysical performance of the MODIS vegetation indices. *Remote Sensing of Environment*, **83**: 195—213

Kim M S. 1994. The Use of Narrow Spectral Bands for Improving Remote Sensing Estimation of Fractionally Absorbed Photosynthetically Active Radiation (fAPAR). Masters Thesis, Department of Geography, University of Maryland, College Park

Li Y M, Ni S X and Wang X Z. 2003. The robustness of linear regression model in rice leaf chlorophyll concentration prediction. *Journal of Remote Sensing*, **9**(5): 364—371

Liu L Y. 2002. Applications of Hyperspectral Remote Sensing In Precision Agriculture. Postdoctoral research work report. Dissertation of Institute of Remote Sensing Application

Pearson R L and Miller L D. 1972. Remote mapping of standing crop biomass for estimation of the productivity of productivity of the short-grass prairie. Pawnee National Grasslands, Colorado. Proceedings of the 8th International Symposium on Remote Sens. Environ., ERIM International.

Pu R L and Gong P. 2000. Hyperspectal Remote Sensing and The Application. High Education Press, Beijing.

Richard B. 2003, EO-1 User Guide v. 2. 3, http://eo1.usgs.gov and http://eo1.gsfs.nasa.gov.

Rouse J W, Haas R H, Schell J A, Deering D W and Harlan J C. 1974. Monitoring the Vernal Advancement of Retrogradation of Natural Vegetation. NASA/GSFC, Type III, Final Report, Greenbelt, MD, USA

Schleicher T D, Bausch W C, Delgado J A and Ayers P D. 2001. Evaluation and refinement of the nitrogen reflectance index (NRI) for site-specific fertilizer management. 2001 ASAE Annual International Meeting. St. Joseph, MI, USA

Shi R H, Niu Z and Zhuang D F. 2005. Research on the effects of leaf biochemical concentrations on leaf spectra: case study of inversion of C:N ratio based on the absorption features centered at 2100nm. *Journal of Remote Sensing*, **9**(1): 1—7

Zhu S P, Chen J, Chen Y Z, He P X and Li Y W. 2000. The prototype research of precision agriculture computer integrated manufacturing system. *Transactions of the CSAE*, **16**(4): 139—141

基于 Hyperion 影像的水稻冠层生化参量反演

陈君颖[1,2], 田庆久[1], 亓雪勇[2], 刘晓臣[1], 管 仲[1]

1. 南京大学 国际地球系统科学研究所, 江苏 南京 210093;
2. 中国资源卫星应用中心, 北京 100073

摘 要: 采用小区实验与大田应用相结合的方法, 依据扬州实验小区地面实测拔节期、抽穗期及灌浆期的水稻叶片、冠层光谱及氮和叶绿素含量, 采用光谱吸收特征和植被指数分析方法, 得到估算水稻氮和叶绿素含量的最佳光谱特征参数; 结合覆盖江苏姜堰地区大田的 Hyperion 高光谱遥感影像, 建立反演水稻冠层氮和叶绿素含量的模型, 对研究区大田水稻冠层氮和叶绿素含量进行了反演及制图。结果表明: 经波深中心归一化方法分析, 发现以 670nm 为中心的光谱吸收特征面积与水稻氮含量呈显著相关性; 基于反转归一化光谱, 结合 560nm 和 670nm 两个波段, 建立的植被指数 NDVI560_670 能很好地反演水稻叶绿素含量。

关键词: 高光谱遥感, 水稻, Hyperion, 氮, 叶绿素

中图分类号: TP79 文献标识码: A

1 引 言

精准农业是当今世界农业发展的趋势, 也是可持续发展农业的重要途径(刘良云, 2002)。它通过 3S 技术的应用, 采集并处理与作物生长有关的环境因素实际存在的空间和时间差异信息, 精细准确地调整各项管理措施, 以获取最高产量和最大经济效益, 同时达到保护环境的目的(祝诗平等, 2000)。

水稻是中国主要的粮食作物之一。生化参量是水稻生长状况的良好指示剂, 如氮含量是指导水稻施肥的重要因素, 叶绿素含量能反映水稻的光合作用情况, 实时监测水稻冠层生化参量的变化, 能及时了解大面积水稻的长势, 是精细农业的重要一环(李云梅等, 2003)。

高光谱遥感具有光谱分辨率高、波段连续性强的特点, 能获得更多的精细光谱信息, 随着高光谱遥感的发展, 为定量分析作物生化参量与光谱特征的关系提供了有力的工具。但目前对于作物生化参量的反演大多数是基于地面采集光谱, 即使应用遥感影像, 也多采用 HyMap、AVIRIS、OMIS 等航空影像。

本研究基于星载高光谱遥感技术, 以精细农业为应用目标, 从不同品种、不同生长条件和不同生育期的水稻叶片、冠层光谱和生化参量数据(氮和叶绿素)分析出发, 研究水稻生育进程中光谱特征和生化参量的相关关系模型, 进而研究水稻冠层生化参量的高光谱遥感信息的定量提取与成图技术。

2 研究区及数据采集

2.1 研究区概况

采用小区实验与大田应用相结合的方法。实验小区(119°24′52.9″E, 32°23′36.9″N)位于扬州大学内, 总面积为 715m^2。扬州市地处江苏中部, 长江北岸, 江淮平原南端, 是江苏省气候生产力较高的区域, 土地垦殖指数较高, 是省内土壤肥力较高地区。实验小区种植了常优 1 号和武粳 15 两个典型水稻品种, 施氮量从不施氮肥到施 25kg 纯氮分为 8 个处理水平, 并种植了两个重复, 共有 32 个小区。

大田即 Hyperion 影像覆盖的地区, 选择在姜堰地区。姜堰自古素有“粮仓”之称, 盛产水稻, 是全国商品粮基地。我们选取了 8 块水稻田作为采样点, 在遥感影像获取的同时进行地面水稻冠层光谱及氮和叶绿素含量的同步测量, 并用 GPS 仪测量了每个采样点的经纬度, 以便在影像上精确定位。图 1 显示了大田影像的覆盖范围和采样点的分布情况。

收稿日期: 2007-06-10; 修订日期: 2008-04-03

基金项目: 江苏省高技术研究项目(编号: BG2004321 和 BG2006340)。

第一作者简介: 陈君颖(1983—), 女, 硕士, 毕业于南京大学主要从事高光谱遥感研究工作, 发表论文 5 篇。E-mail: cjy831025@163.com。

图 1 姜堰大田影像覆盖范围及采样点分布图

2.2 地面光谱测量

水稻反射率光谱的采集使用的是美国 ASD 公司的 FieldSpec Pro FR 光谱仪，波长范围为 350—2500nm，采样间隔在 350—1000nm 范围内为 1.4nm，在 1000—2500nm 范围内为 2nm。

水稻冠层光谱测量是在天气晴朗、少云的情况下，使用光谱仪 25°前视场，探头距水稻冠层 0.5m 左右，探头方向垂直于冠层进行。对每个小区设定 3—5 个样点，对每个样点采集 2—3 条光谱曲线，将每个小区的采集的光谱曲线进行平均得到每个小区的冠层光谱。

在扬州实验田每小区采集 5 片倒三叶叶片，在姜堰每块大田采集 10 片倒三叶叶片作为样本进行水稻叶片光谱的测量。测量是在暗室内进行，对每个叶片测量 4—6 条反射率光谱曲线，取其平均值作为每片叶片的光谱。

从 2005 年 8 月 15 日至 9 月 30 日，经历了水稻的拔节期、抽穗期和灌浆期 3 个生长期，共采集了 1225 条冠层光谱和 2925 条叶片光谱。如表 1，在扬州实验小区分别于 2005 年 8 月 15 日、9 月 6 日和 9 月 30 日进行了 3 次冠层、叶片反射率光谱的测量。在姜堰的大田于 2005 年 9 月 7 日与卫星遥感影像获取同步进行了地面水稻冠层光谱的测量，获取了 8 个采样点的冠层反射率光谱。

表 1 2005 年地面光谱采集情况

日期	8 月 15 日	9 月 6 日	9 月 7 日	9 月 30 日
地点	扬州实验小区	扬州实验小区	姜堰大田	扬州实验小区
生育期	拔节期	抽穗期	抽穗期	灌浆期
样本数/个	160	192	—	160
冠层光谱数/个	324	289	128	484
叶片光谱数/个	960	1000	—	965

2.3 氮和叶绿素含量的采集与处理

在水稻光谱测量后立即对样本进行了氮和叶绿素含量的测量。氮含量的测量采用凯氏定氮法。叶绿素含量的测量使用美能达 SPAD-502 叶绿素测量仪。SPAD-502 叶绿素测量仪是日本产的一种小巧的对植物无破坏性的叶绿素含量测定仪，它通过测定植物叶子在两个波长区的吸收率确定叶子叶绿素浓度的相对含量(浦瑞良等, 2000)。对每个叶片测量叶绿素含量 6—10 次，取其平均值作为每个叶片的叶绿素含量。每小区所有叶片样本的氮和叶绿素含量的平均值作为该小区相应的冠层氮和叶绿素含量值。

2.4 Hyperion 高光谱遥感数据获取

Hyperion 是第一个星载民用成像光谱仪，它是以推扫方式获取可见光、近红外(VNIR)和短波红外(SWIR)光谱数据，共有 242 个波段，其主要技术参数见表 2。

2005 年 9 月 7 日上午 10 点 20 分获取了覆盖江苏省姜堰市地区的 Hyperion 高光谱遥感影像。影像中心点的经纬度为 120°8′2″E，32°29′6″N，大小为 255×3471 像元。

表 2 Hyperion 数据主要技术参数(Richard, 2003)

波长范围/nm	356—2577
波段数	242
空间分辨率/m	30
VNIR 波段	1—70(356—1058nm)
SWIR 波段	71—242(852—2577nm)
数据类型	2 位有符号整型

3 Hyperion 数据处理

3.1 Hyperion 数据预处理

Hyperion 数据预处理经过未定标及受水汽影响波段的去除、绝对辐射值的转换、条纹及 Smile 效应去除、大气校正和光谱平滑去噪，最后得到 Hyperion 反射率影像。

将未定标、受水汽影响和噪声较大的波段去除后，本研究最终使用了 166 个波段，保留的波段及其波长范围见表 3。

将所有 VNIR 波段除以 40，生成一个新影像文件，然后将所有 SWIR 波段除以 80，生成另一个新影

表 3 保留的 **Hyperion** 影像波段

Hyperion 原始波段	波长范围/nm
8—54	426—895
80—119	943—1336
131—164	1457—1790
180—224	1952—2396

像文件，将两个影像文件合并，得到绝对辐射值影像。

条纹及 Smile 效应去除是采用全局均衡法。其原理是认为 Hyperion 每个波段图像每一列数据的均值和标准差是一致的，然后以整幅图像的均值和标准差为标准来修正图像中每一列数据的均值和标准差。

采用 Fast Line-of-sight Atmospheric Analysis of Spectral Hypercubes(FLAASH)模块对 Hyperion 影像进行大气订正，得到反射率影像。FLAASH 是一个第一定理大气纠正模型，它用来从高光谱影像得到光谱反射率。它能较好地消除大气造成的模糊效应。

由于经过一系列的处理，每个环节有一定缺陷和不确定性，产生冗余的信息，导致大气纠正后的反射率影像的像元光谱大部分具有连续的锯齿噪音，对影像的定量化应用产生不利影响，所以本研究采用了一种影像 MNF 转换的方法对影像光谱曲线进行平滑去噪(Datt 等, 2003)。

预处理后的影像反射率光谱曲线与同一地区田间测量的冠层反射率光谱曲线十分类似(图 2)，地物光谱重建效果很好。

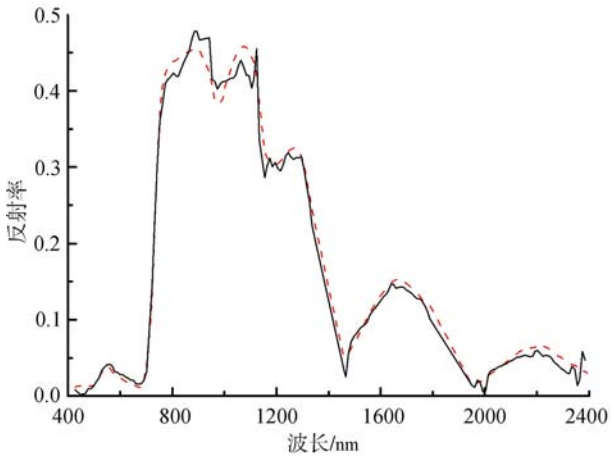

图 2 Hyperion 影像反射率光谱(实线)和田间测量冠层重采样光谱(虚线)对比

3.2 几何校正

以影像覆盖区域内 1 5 万的地形图为基准，采用人机交互选择了 22 个地面控制点，利用二次多项式和双线性内插法对 Hyperion 反射率影像进行几何纠正，总误差控制在一个像元内。

3.3 水稻区提取

由于本实验的研究目标是水稻，为了使结果更容易判读，我们将水稻区从影像上提取出来以便于对研究区内水稻生化参量进行针对性的分析和反演制图。

首先根据归一化植被指数(NDVI)将植被区域提取出来，它定义为近红外波段与可见光红波段数值之差和这两个波段数值之和的比值。即:

$$\mathrm{NDVI}=\frac{\rho_{\mathrm{NIR}}-\rho_{\mathrm{RED}}}{\rho_{\mathrm{NIR}}+\rho_{\mathrm{RED}}} \tag{1}$$

式中，ρ_{RED} 和ρ_{NIR} 分别是红光和近红外波段的反射率。本研究将 NDVI≥0.7 的区域提取为植被。

然后计算了影像的优化植被指数 (EVI)和表面水指数(LSWI)(Huete 等, 2002)。它们的计算公式如下:

$$\mathrm{EVI}=2.5\times\frac{\rho_{\mathrm{NIR}}-\rho_{\mathrm{RED}}}{\rho_{\mathrm{NIR}}+6\times\rho_{\mathrm{RED}}-7.5\times\rho_{\mathrm{BLUE}}+1} \tag{2}$$

$$\mathrm{LSWI}=\frac{\rho_{\mathrm{NIR}}-\rho_{\mathrm{SWIR}}}{\rho_{\mathrm{NIR}}+\rho_{\mathrm{SWIR}}} \tag{3}$$

式中，ρ_{BLUE}、ρ_{RED}、ρ_{NIR} 和ρ_{SWIR} 分别是蓝光、红光、近红外和短波红外波段的反射率。由于影像获取的时间为 9 月 7 日，水稻处于抽穗期，叶面积指数较大，而当植被覆盖度大于 80%时，其 NDVI 值增加延缓呈现饱和状态，对植被检测灵敏度下降，所以为了将水稻与其他植被更好地区别，我们采用了 EVI，它用蓝光波段对红光波段进行调整，对大气污染、土壤及冠层背景更为敏感(Huete 等, 1997, 2002)。相比较其他植被类型，水稻的 EVI 值较其他植被类型小。水稻区别于其他植被的显著特征是种植在水中，我们采用了对叶片含水量和土壤湿度非常敏感 LSWI。对于水稻，其 LSWI 要大于其他植被类型。因此对于水稻区，其 EVI–LSWI 值较其他植被类型低。本研究将 EVI–LSWI≤0.24 的区域提取出来作为水稻区。

图 3 显示了原始假彩色合成影像与提取出水稻区的对比。从图 3(a)原始假彩色合成影像中看出由于受水背景的影响，水稻显示为暗红色，而其他植被类型显示为较明亮的红色。图 3(b)中白色区域为水稻田。对水稻区提取结果进行了精度评价，选取了 3812 个非植被样本、272 个水稻样本和 2483 个其他植被样本，建立混淆矩阵，计算相关指标，得到精度评价结果(表 4)。从表 4 可知，水稻区提取的总体精度达到了 92.89%, Kappa 系数为 0.8915，证明该提取水稻方法具有较高的准确性和可行性。

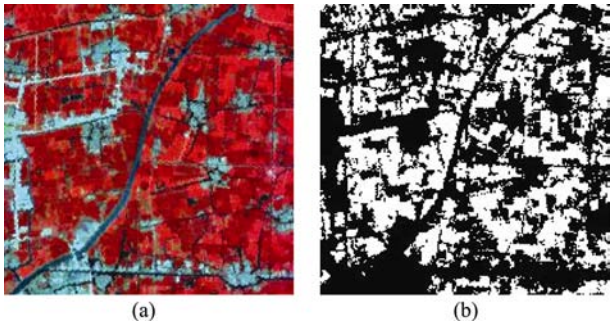

图 3 原始假彩色合成影像与提取出水稻区图像对比
(a)原始假彩色合成影像; (b)水稻区图

表 4 水稻区提取分类精度评价

类型	非植被	水稻	其他植被	总和	使用者精度/%
非植被	3701	16	15	3732	99.17
水稻	70	2563	353	2986	85.83
其他植被	41	146	2115	2302	91.88
总和	3812	2725	2483	9020	—
生产精度/%	97.09	94.06	85.18	—	—
总精度＝92.89%			Kappa 系数＝0.8915		

4 研究方法

4.1 基于光谱吸收特征的分析方法

基于连续统去除(Continuum Removal)能突出吸收特征并减少背景影响。首先在吸收中心两侧确定两个相对峰值点作为端点，连接两个端点构成一条包络在反射曲线上方的直线，称为连续统。连续统去除后的相对反射率就是用实际光谱反射率除以连续统上相应波长处的反射率(施润和等, 2005)。在连续统去除的基础上，采用了波深中心归一化和波段面积归一化两种光谱变化形式。

4.1.1 波深中心归一化(BNC)

用各波段波深除以吸收特征中心波长对应的波深值，计算公式如下:

$$\mathrm{BNC}=(1-(R/R'))/(1-(R_c/R_c')) \quad (4)$$

式中，R 为各波长对应的反射率，R'为各波长在包络线上的反射率，R_c 为吸收特征中心波长对应的反射率，R_c'为吸收中心波长在包络线上的反射率。

4.1.2 波段面积归一化(BNA)

用各波段波深除以吸收特征面积，计算公式为:

$$\mathrm{BNA}=(1-(R/R'))/A \quad (5)$$

式中，A 为包络线去除后吸收特性面积。

4.1.3 光谱吸收特征波段选择

研究中使用了 2 种波段选择方法:

(1) 对每个样本的整条光谱曲线进行包络线去除。如图 4、图 5，经包络线去除后的光谱曲线产生了 4 个独立的波段区间，分别以 670、980、1160 和 1950nm 为中心。

(2) 根据水稻原始反射率光谱和已知的氮素和叶绿素吸收特征，我们选取了 6 个大的吸收特征区间(表 5)。已知的氮素和叶绿素吸收特征参照

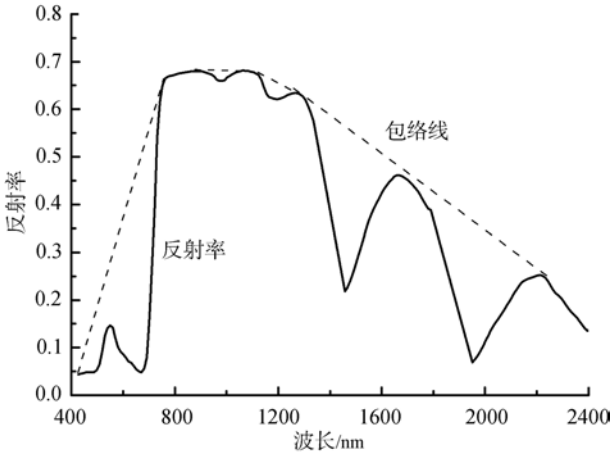

图 4 反射率光谱曲线及其包络线示意图

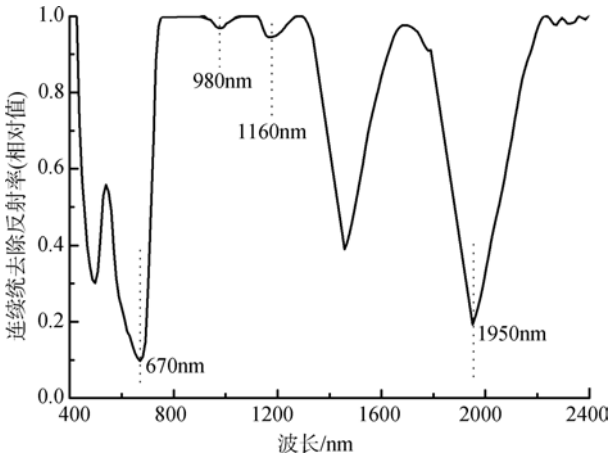

图 5 连续统去除后光谱曲线及光谱吸收中心

表 5 入选氮素和叶绿素吸收特征位置及波段范围

已知氮素和叶绿素吸收特征/nm	波段范围/nm
460	436.99—548.92
640, 660	569.27—762.6
910, 1020	894.7—1083.99
1510	1285.76—1648.91
1980, 2060, 2130, 2180	1961.66—2203.83
2240, 2300, 2350	2224.02—2395.5

了 Curran(1989)等对干叶捣碎后的光谱吸收特征测定结果：氮素的吸收特征中心分别位于 910、1020、1510、1980、2060、2130、2180、2240、2300 和 2350nm，叶绿素的吸收特征中心分别位于 460、640 和 660nm。

在对光谱进行了波深中心归一化和波段面积归一化变换后，分别求取了各吸收特征的深度、宽度和面积，计算了它们与氮和叶绿素含量的相关关系。

4.2 基于植被指数的研究方法

根据水稻光谱特征和参考文献，挑选了 6 种植被指数如表 6。对原始光谱进行了连续统去除得到归一化光谱，用 1 减去归一化后的光谱，得到反转的归一化光谱，再基于原始光谱、归一化光谱和反转归一化光谱分别计算了这 6 种植被指数与氮和叶绿素含量的相关关系。

5 结果分析

5.1 水稻氮和叶绿素含量估算最佳光谱特征参数选择

对 8 月 15 日拔节期、9 月 6 日抽穗期和 9 月 30 日灌浆期 3 次地面采集的水稻叶片、冠层光谱及相应氮和叶绿素含量进行了统计相关分析，计算了各光谱吸收特征参数和植被指数与氮和叶绿素含量的相关系数。

在 3 个生育期、冠层和叶片两种尺度，与氮含量成显著相关的参数如表 7。其中相关系数最高的参数为光谱变化为波深中心归一化形式，以 670nm 为中心的吸收特征面积，即 670Area(BNC)，因此在本研究中选用此参数作为估算水稻氮含量的最佳光谱特征参数。

在 3 个生育期、冠层和叶片两种尺度，与叶绿素含量成显著相关的参数如表 8。其中相关系数最

表 6 选用的植被指数

植被指数	全称	计算公式	参考
NDVI560_670	Normalized difference vegetation index	$\mathrm{NDVI560\_670}=\frac{R_{560}-R_{670}}{R_{560}+R_{670}}$	Rouse 等,1974
RVI560_670	Ratio vegetation index	$\mathrm{RVI560\_670}=\frac{R_{560}}{R_{670}}$	Pearson&Miller, 1972
NRI	Nitrogen reflectance index	$\mathrm{NRI}=\frac{R_{570}-R_{670}}{R_{570}+R_{670}}$	Schleiche 等, 2001
CARI	Chlorophyll absorption ratio index	$\mathrm{CARI}=\frac{\lvert a\times 670+R_{670}+b\rvert R_{700}}{\sqrt{a^2+1}\times R_{670}}$, $a=(R_{700}-R_{550})/150, b=R_{550}-550\times a$	Kim 等, 1994
VARI_green	Visible atmospherically resistant index	$\mathrm{VARI\_green}=\frac{R_{560}-R_{670}}{R_{560}+R_{670}+R_{450}}$	Anatoly 等, 2002
VARI_700	Visible atmospherically resistant index	$\mathrm{VARI\_700}=\frac{R_{700}-1.7\times R_{670}+0.7\times R_{450}}{R_{700}+2.3\times R_{670}-1.3\times R_{450}}$	Anatoly 等, 2002

表 7 与氮含量成显著相关的光谱特征参数及其复相关系数(R^2)(2005 年)

光谱特征参数	8 月 15 日		9 月 6 日		9 月 30 日	
	叶片	冠层	叶片	冠层	叶片	冠层
PSSRb(原始光谱)	0.55	0.55	0.56	0.44	0.74	0.61
PSNDb(原始光谱)	0.55	0.56	0.61	0.50	0.74	0.71
CARI(归一化光谱)	0.67	0.61	0.62	0.52	0.77	0.74
NDVI560_670(反转归一化光谱)	0.71	0.56	0.61	0.55	0.72	0.72
RVI560_670(反转归一化光谱)	0.71	0.58	0.61	0.55	0.76	0.74
NRI(反转归一化光谱)	0.69	0.58	0.62	0.56	0.72	0.72
CARI(反转归一化光谱)	0.67	0.59	0.62	0.48	0.77	0.72
VARI_green(反转归一化光谱)	0.69	0.56	0.61	0.53	0.72	0.72
VARI_700(反转归一化光谱)	0.69	0.55	0.66	0.49	0.76	0.74
670Area(BNC)	0.72	0.56	0.62	0.56	0.76	0.74
670Depth(BNA)	0.66	0.56	0.64	0.50	0.71	0.72
640, 660Depth(BNA)	0.64	0.61	0.49	0.55	0.83	0.74

表 8 与叶绿素含量成显著相关的光谱特征参数及其复相关系数(R^2)(2005 年)

光谱特征参数	8 月 15 日		9 月 6 日		9 月 30 日	
	叶片	冠层	叶片	冠层	叶片	冠层
PSNDb(原始光谱)	0.64	0.56	0.62	0.44	0.94	0.77
CARI(归一化光谱)	0.71	0.67	0.66	0.53	0.96	0.85
NDVI560_670(反转归一化光谱)	0.76	0.62	0.71	0.58	0.96	0.86
RVI560_670(反转归一化光谱)	0.76	0.59	0.71	0.58	0.96	0.85
NRI(反转归一化光谱)	0.76	0.62	0.71	0.56	0.96	0.86
CARI(反转归一化光谱)	0.74	0.62	0.61	0.48	0.94	0.83
VARI_green(反转归一化光谱)	0.76	0.61	0.72	0.56	0.96	0.86
VARI_700(反转归一化光谱)	0.76	0.53	0.66	0.48	0.96	0.85
670Depth(BNA)	0.74	0.58	0.71	0.52	0.96	0.86
640, 660Area(BNC)	0.76	0.61	0.67	0.48	0.94	0.79
640, 660Depth(BNA)	0.76	0.64	0.67	0.49	0.96	0.83

高的参数为基于反转归一化光谱形式，结合 560nm 和 670nm 波段计算的植被指数 NDVI，即 NDVI560_670(反转归一化光谱)，因此在本研究中选用此参数作为估算水稻叶绿素含量的最佳光谱特征参数。

5.2 基于 Hyperion 影像的水稻冠层氮和叶绿素含量反演及制图

基于 Hyperion 反射率影像，将上述地面采集数据研究结果运用到经田间同步测量的 8 块大田影像光谱及其相应的冠层氮和叶绿素含量中，建立了研究区水稻冠层氮和叶绿素含量的反演模型如式(6)、式(7)。670Area(BNC)与水稻冠层氮含量的复相关系数(R^2)达 0.79，NDVI560_670(反转归一化光谱)与水稻冠层叶绿素含量的 R^2 为 0.77，精度较高(图 6、图 7)。

$$N = 0.0357 \times 670\text{Area(BNC)} - 7.0023 \quad (6)$$

CHL=207.16×NDVI560_670(反转归一化光谱)+15.772 (7)

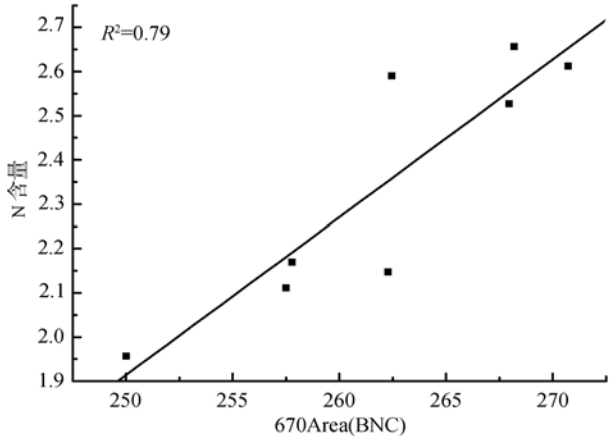

图 6 影像光谱 670Area(BNC)与氮含量的相关性

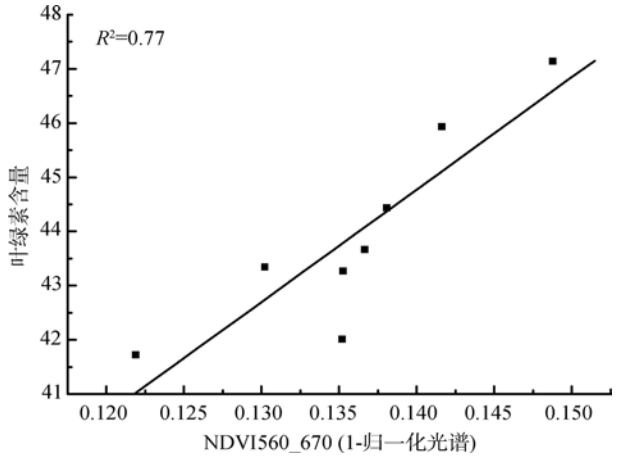

图 7 影像光谱 NDVI560_670(反转归一化光谱)与冠层叶绿素含量的相关性

将反演模型运用到整幅提取出水稻区的 Hyperion 影像上，得到研究区的水稻冠层氮和叶绿素含量分布图(图 8、图 9)，图像上冠层氮含量的值域为 0.06%－4.46%，冠层叶绿素含量的值域为 31.04—68.44，与地面的分析结果基本一致，且单块田的值也较为统一，氮和叶绿素含量的大小分布与水稻长势分布一致，这在一定程度上说明反演模型的有效性。

6 结论与展望

通过分析小区采集的不同品种水稻不同生育期的叶片和冠层反射率光谱特征与水稻氮和叶绿素含量的相关关系，获得具有一定普适性、精度较高的估算水稻氮和叶绿素含量的光谱特征参数，进而将小区地面数据研究结果运用到覆盖大田的 Hyperion 高光谱遥感影像上，建立了反演水稻冠层氮和叶绿

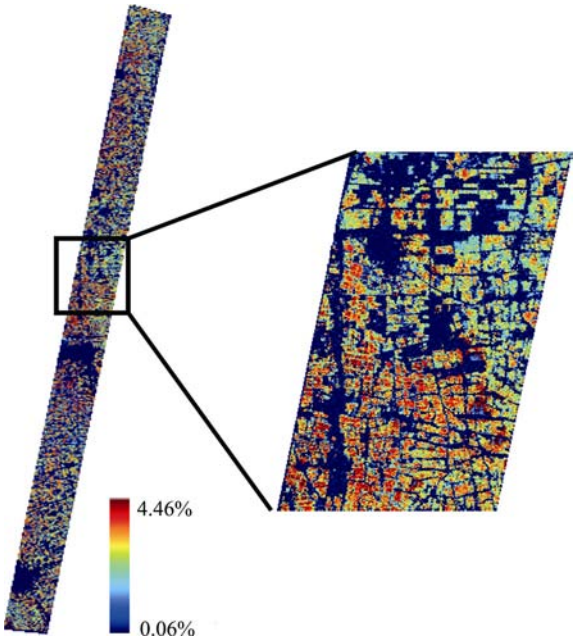

图 8 研究区水稻冠层氮含量分布图

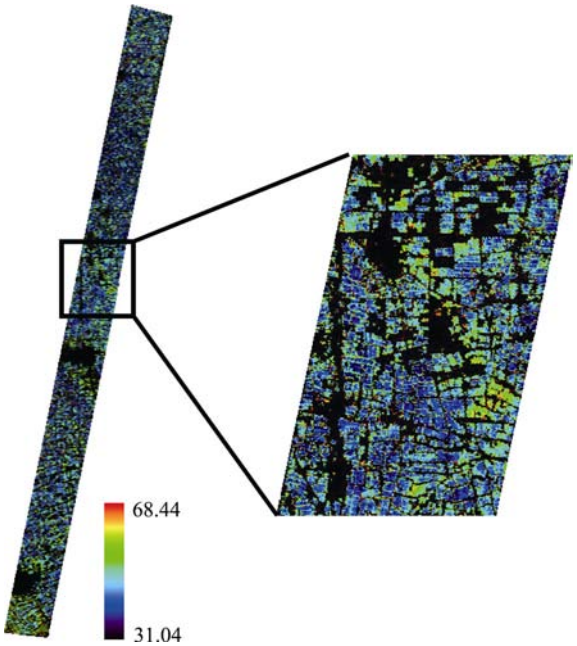

图 9 研究区水稻冠层叶绿素含量分布图

素含量的模型，探讨了基于 Hyperion 影像反演水稻冠层氮和叶绿素含量的可行性，并对研究区的水稻冠层氮和叶绿素含量进行反演，最后制成研究区水稻冠层氮和叶绿素含量分布图。结果表明:

(1) 经波深中心归一化方法分析，发现以 670nm 为中心的光谱吸收特征面积在拔节、抽穗和灌浆 3 个生育期，叶片、冠层 2 种尺度均与氮含量呈显著相关关系，能很好地反演水稻氮含量。基于星载高光谱遥感影像建立了研究区水稻冠层氮含量反演模型，结果表明，影像光谱经波深中心归一化变化得到的以 670nm 为中心的光谱吸收面积与水稻冠层氮含量的复相关系数(R^2)达 0.79，反演结果精确可靠。

(2) 采用反转归一化光谱变化形式，结合 560nm 和 670nm 两个波段，建立了植被指数 NDVI560_670，该光谱特征参数在拔节、抽穗和灌浆 3 个生育期，叶片、冠层 2 种尺度均与水稻叶绿素含量呈显著相关性。基于星载高光谱遥感影像建立了研究区水稻冠层叶绿素含量反演模型，结果表明，基于影像反转归一化光谱的 NDVI560_670 与水稻冠层叶绿素含量的 R^2 达 0.77，精度较高，结果令人满意。

本研究主要以水稻为研究对象，探讨了反演氮和叶绿素含量的方法，今后可将研究对象扩展到其他植被类型和更多生物理化参量。研究提出的方法还可为今后高光谱遥感在作物估产、病虫害检测中的研究提供借鉴。

REFERENCES

Anatoly A, Gitelson Y, Yoram J K, Robert S and Don R. 2002. Novel algorithms for remote estimation of vegetation fraction. *Remote Sens. Environ*, **80**: 76—87

Curran P J. 1989. Remote sensing of foliar chemistry. *Remote Sensing of Environment*, **30**, 271—278

Datt B, McVicar T R, Van Niel T G, Jupp D L B and Pearlman J S. 2003. Pre-processing EO-1 hyperion hyperspectral data to support the application of agricultural indices. *IEEE Transactions on Geoscience and Remote Sensing*, **41**(6): 1246—1259

FLAASH Module User's Guide, ENVI FLAASH Version 4.2, August, 2005 Edtion

<http://www.jsyzagri.gov.cn/old/gkzr.htm.>

<http://jiangyan.soujz.com/.>

Huete A R, Liu H Q, Batchily K and VanLeeuwen W. 1997. A comparison of vegetation indices global set of TM images for EOSMODIS. *Remote Sensing of Environment*, **59**: 440—451

Huete A R, Didan K, Miura T, Rodriguez E P, Gao X and Ferreira L G. 2002. Overview of the radiometric and biophysical performance of the MODIS vegetation indices. *Remote Sensing of Environment*, **83**: 195—213

Kim M S. 1994. The Use of Narrow Spectral Bands for Improving Remote Sensing Estimation of Fractionally Absorbed Photosynthetically Active Radiation (fAPAR). Masters Thesis, Department of Geography, University of Maryland, College Park

Li Y M, Ni S X and Wang X Z. 2003. The robustness of linear regression model in rice leaf chlorophyll concentration prediction. *Journal of Remote Sensing*, **9**(5): 364—371

Liu L Y. 2002. Applications of Hyperspectral Remote Sensing In Precision Agriculture. Postdoctoral research work report. Dis-

sertation of Institute of Remote Sensing Application

Pearson R L and Miller L D. 1972. Remote mapping of standing crop biomass for estimation of the productivity of productivity of the short-grass prairie. Pawnee National Grasslands, Colorado. Proceedings of the 8th International Symposium on Remote Sens. Environ., ERIM International.

Pu R L and Gong P. 2000. Hyperspectal Remote Sensing and The Application. High Education Press, Beijing.

Richard B. 2003, EO-1 User Guide v. 2. 3, http://eo1.usgs.gov and http://eo1.gsfs.nasa.gov.

Rouse J W, Haas R H, Schell J A, Deering D W and Harlan J C. 1974. Monitoring the Vernal Advancement of Retrogradation of Natural Vegetation. NASA/GSFC, Type III, Final Report, Greenbelt, MD, USA

Schleicher T D, Bausch W C, Delgado J A and Ayers P D. 2001. Evaluation and refinement of the nitrogen reflectance index (NRI) for site-specific fertilizer management. 2001 ASAE Annual International Meeting. St. Joseph, MI, USA

Shi R H, Niu Z and Zhuang D F. 2005. Research on the effects of leaf biochemical concentrations on leaf spectra: case study of inversion of C:N ratio based on the absorption features centered at 2100nm. *Journal of Remote Sensing*, **9**(1): 1—7

Zhu S P, Chen J, Chen Y, He P X and Li Y W. 2000. The prototype research of precision agriculture computer integrated manufacturing system. *Transactions of the CSAE*, **16**(4): 139—141

附中文参考文献

李云梅, 倪绍祥, 王秀珍. 2003. 线性回归模型估算水稻叶片叶绿素含量的适宜性分析. 遥感学报, **9**(5): 364—371

刘良云. 2002. 高光谱遥感在精准农业中的应用研究. 博士后研究工作报告. 中国科学院遥感应用研究所

浦瑞良, 宫鹏. 2000. 高光谱遥感及其应用. 北京: 高等教育出版社

施润和, 牛铮, 庄大方. 2005. 叶片生化组分浓度对单叶光谱影响研究——以 2100nm 吸收特征的碳氮比反演为例. 遥感学报, **9**(1): 1—7

祝诗平, 陈建, 陈 , 何培祥, 李云伍. 2000. 精细农业计算机集成制造系统原型研究. 农业工程学报, **16**(4): 139—141